Structural Characterization of Nonionic Mixed Micelles Formed by C12EO6 Surfactant and P123 Triblock Copolymer

5 AUTHORS, INCLUDING:

Matija Tomsic
University of Ljubljana
40 PUBLICATIONS **520** CITATIONS

SEE PROFILE

Karin Schillén
Lund University
80 PUBLICATIONS **2,865** CITATIONS

SEE PROFILE

Structural Characterization of Nonionic Mixed Micelles Formed by $C_{12}EO_6$ Surfactant and P123 Triblock Copolymer

David Löf,[†,‡] Matija Tomšič,[∥] Otto Glatter,[§] Gerhard Fritz-Popovski,[§] and Karin Schillén*,[†]

Division of Physical Chemistry, Center for Chemistry and Chemical Engineering, P.O. Box 124, Lund University, SE-22100 Lund, Sweden, Faculty of Chemistry and Chemical Technology, University of Ljubljana, Aškerčeva 5, SI-1001 Ljubljana, Slovenia, and Institute of Chemistry, University of Graz, Heinrichstrasse 28, A-8010 Graz, Austria

A structural characterization of mixed micelles formed in aqueous solution by the PEO-PPO-PEO triblock copolymer P123 and the nonionic surfactant $C_{12}EO_6$ was carried out using various techniques, including ultralow shear viscosimetry, depolarized dynamic light scattering (VH-DLS), depolarized static light scattering (VH-SLS), and small-angle X-ray scattering (SAXS). The sphere-to-rod transition of the mixed micelles was studied in a diluted regime (P123 concentrations ranging from 0.5 to 10 wt %) at $C_{12}EO_6$/P123 molar ratios of 2.2, 3.2, 6.0, and 11 as well as for the pure $C_{12}EO_6$. The data from VH-SLS and viscosimetry displayed a sharp increase in the intensity and viscosity, respectively, at the sphere-to-rod transition, and the results from the two methods were in accordance. In both techniques, an increased transition temperature with increasing content of $C_{12}EO_6$ (in the molar ratio regime from 2.2 to 11) was observed. SAXS was used as the main technique, and a thorough structural characterization was performed, where indirect Fourier transformation (IFT) and generalized indirect Fourier transformation (GIFT) were employed in the analysis procedure of the SAXS data. The $p(r)$ functions obtained from the IFT (employed at low P123 concentrations, i.e., 1.0 and 2.0 wt %) and GIFT (employed above 2.0 wt %) analyses revealed increased inhomogeneities in the mixed micelles when the molar ratio was increased. This suggested that the $C_{12}EO_6$ organized themselves at the interface between the PPO core and the PEO corona of the P123 micelles, with the C_{12} alkyl chain stretching into the hydrophobic core and the EO_6 part residing in the hydrophilic corona. The structure factor parameters obtained with GIFT for a molar ratio of 2.2 at a P123 concentration of 5.0 wt % showed radius values smaller than what was estimated from the $p(r)$ functions. This was explained by an interpenetration of the PEO chains from one mixed micelle into a neighboring one. VH-DLS was performed on the mixed micelles at a temperature 3 °C above the transition temperature and at a molar ratio of 2.2. From the analyzed data, the average length L of the rods was estimated to be 102 nm.

Introduction

The self-assembly in water of nonionic amphiphiles such as triblock copolymers of poly(ethylene oxide) (PEO) and poly(propylene oxide) (PPO) in the form PEO-PPO-PEO and C_iEO_j surfactants has been extensively studied during the last decades. The interest in this topic has its origin in the scientific field but also in industrial applications of, e.g., the PEO-PPO-PEO copolymers,[1−3] where such amphiphiles are used as detergents and emulsifiers and for controlled delivery purposes in pharmaceutical products.[4,5] Due to their synergistic behavior, PEO-PPO-PEO copolymers and surfactants—both ionic and nonionic—are often mixed together in solutions. There are numerous studies in the literature focusing on the interactions between various kinds of triblock copolymers mixed with ionic surfactants in water.[6−19] Fewer studies have been published on mixtures with nonionic surfactants, see e.g., refs 20, 18, and 21. In previous investigations, our group has explored dilute solutions of the $EO_{20}PO_{68}EO_{20}$ copolymer P123 and the nonionic

surfactant $C_{12}EO_6$ and determined their interaction as well as the formation of mixed micelles by means of calorimetry and light scattering techniques.[22,23] These studies led to the observation of a new phenomenon, namely, that the mixed micelles underwent a sphere-to-rod transition at a well-defined temperature that varied according to the $C_{12}EO_6$/P123 molar ratio.[22] The shape transition temperature presented a minimum at a molar ratio between 2 and 3 and followed the same trend as the phase separation temperature at higher temperature. This shape transition was attributed to the PEO conformation change in the corona induced by the surfactants. Additionally, when the molar ratio was increased above 3, the spherical micelles decreased in size and the sphere-to-rod transition temperature increased again. This was explained by the larger amount of energy required by the system, due to the higher curvature of the smaller micelles, in order to change the micellar shape. This was also confirmed in a rheological study of the same system.[24] Recently, the investigation has also been extended to include higher $C_{12}EO_6$/P123 molar ratios in order to understand the effect of the composition on the micellar structure. Here, the experimental techniques were static light scattering (SLS) and dynamic light scattering (DLS),[23] and we found a composition-induced structural change at constant temperature, which was manifested in the intermicellar interaction. The mixed micelles

* To whom correspondence should be addressed. E-mail: Karin.Schillen@fkem1.lu.se. Fax: +46 46222 4413. Tel.: +46 46222 1439.
† Lund University.
‡ Present address: Dyrup A/S, Gladsaxevej 300, DK-2860 Soeborg, Denmark.
§ University of Graz.
∥ University of Ljubljana.

changed from being spherical at low $C_{12}EO_6$/P123 molar ratios to polymer-like ("wormlike") at high molar ratios.

The present work aims at further investigating the shape of the P123−$C_{12}EO_6$ mixed micelles in the low molar ratio regime, where the temperature-induced sphere-to-rod transition occurs. This is done with the objective to understand the process of transition from a molecular point of view and to confirm the rodlike character of the mixed micelles after the transition. Various $C_{12}EO_6$/P123 molar ratios have been investigated at different total concentrations, with an emphasis on a molar ratio of 2.2. Three techniques have been used in order to characterize the P123−$C_{12}EO_6$ mixed micellar system; a DMA densiometer (density measurement apparatus) was utilized to achieve information concerning the viscosity in the solutions; the rotational motion of the rodlike mixed micelles was characterized by depolarized (VH) dynamic light scattering enabling a determination of the length; and depolarized scattering intensity (I_{VH}) measurements were also performed as functions of temperature for various $C_{12}EO_6$/P123 molar ratios. Small-angle X-ray scattering (SAXS) was the main technique employed in order to characterize the shape and the physical properties of the mixed micelles, and indirect Fourier transformation (IFT) and generalized indirect Fourier transformation (GIFT) techniques were used to analyze the SAXS data.

Experimental Section

Materials. The PEO-PPO-PEO triblock copolymer (denoted P123) has an average composition of $EO_{20}PO_{68}EO_{20}$ and a nominal molar mass of 5750 g mol^{-1}.[25] The sample was generously donated by BASF Corporation, Performance Chemicals, Mount Olive, NJ, and was used without further treatment. It is well-known that the PEO-PPO-PEO copolymers are polydisperse both in molar mass and composition,[13,26−28] and recently a study of the effect of diblock impurities on the structural properties of ordered PEO-PPO-PEO micellar phases has been reported.[29] The critical micelle concentration (cmc) of P123 may vary between different sample batches of different polydispersity and the experimental technique used. We have previously estimated the cmc at 40 °C to be 0.2×10^{-3} wt % (or 3.47×10^{-7} mol L^{-1}) by using isothermal titration calorimetry (ITC)[11,13] and 1.8×10^{-6} mol L^{-1} by using steady-state fluorescence spectroscopy.[30] Wanka et al. has reported a value of 5.2×10^{-7} mol L^{-1}.[31] For a 1.0 wt % P123 solution, the critical micelle temperature is 17 ± 1 °C and the liquid−liquid phase separation temperature is 79 °C according to DSC experiments.[22] Hexa(ethylene glycol) monododecyl ether ($C_{12}EO_6$) was obtained from Nikko Chemicals Co., Tokyo, Japan, and used as received. Its molar mass was 450.7 g mol^{-1}. According to the gas chromatogram provided by the manufacturer, the purity of the sample was superior to 99%. The cmc of $C_{12}EO_6$ at 40 °C is 5.3×10^{-5} mol L^{-1} as determined using ITC,[32] and the critical point for the liquid−liquid phase separation in a 2.25 wt % $C_{12}EO_6$ solution is about 47 °C.[33] Water purified by a Milli-Q system (Millipore Corporation, Bedford, MA) was used in all solutions. The stock solutions of the P123 and $C_{12}EO_6$ were prepared by weighing and left to equilibrate overnight in a refrigerator at 4 °C. The mixed micellar solutions were prepared at various $C_{12}EO_6$/P123 molar ratios defined as the ratio between the number of moles of $C_{12}EO_6$ and P123. All samples were equilibrated at room temperature prior to the measurements.

Ultralow Shear Viscosimetry. The viscosities of the micellar solutions were determined by utilizing a DMA 5000 (Anton Paar KG, Graz, Austria). This instrument consists of an oscillating tube and is principally a density meter. The effects from the viscosity lead to certain errors in the density measurements, and the measured densities thus have to be corrected for these effects. The sample viscosity causes a damping of the oscillating tube, and the corresponding signals are used for these corrections. Furthermore, the signals can be converted so as to become viscosity-dependent (a detailed description is given in ref 34) and thereby render the possibility of monitoring the changes in the sample viscosity at extremely low shear rates. All the P123−$C_{12}EO_6$ solutions that were studied with this technique were prepared to 5.0 wt % with respect to P123; i.e., the concentration of P123 [$c_{P123} = m_{P123}/(m_{P123} + m_{C12EO6} + m_{water}) \times 100$ wt %] was kept constant. Approximately 1.0 mL of the solution was injected into the DMA instrument, whereupon the temperature was set. Measurements were performed on a series of temperatures with increments of 1 °C, and, in order to let the system reach thermal equilibrium, the measurements started 30 min after the set temperature for the scanning procedure was reached. The starting temperature was chosen to 25 °C for all measurements, whereas the final temperature varied from 50 to 75 °C depending on the molar ratio so as to cover the transition temperature in each case.

Depolarized Light Scattering. Both static and dynamic depolarized light scattering (VH-SLS and VH-DLS) measurements were carried out using a laboratory-built precision laser goniometer (Institute of Chemistry, University of Graz, Austria), equipped with a 5 W single frequency solid-state diode-pumped laser with a wavelength $\lambda = 532$ nm, Coherent, model Verdi, and two, high quality, Glan-Thompson polarizers (Halle, Berlin, Germany) with extinction ratios $>10^{-6}$. The cylindrical light scattering cells (cuvettes with inner diameters of 8 mm) were immersed in a refractive-index-matching liquid (*cis*-decahydronaphthalene or decaline) kept in a cylindrical quartz container (VAT). The first polarizer was located in front of the VAT, and the second (the analyzer) in front of the detector. In order to measure the depolarized light scattering, the second polarizer was rotated 90° relative to the first one. The laser operated at an effective power of 1 W. The VH-SLS measurements were performed at the scattering angle $\theta = 90°$ relative to the direction of the primary beam, whereas the VH-DLS experiments used angles from 35° to 135° with a step width of 5°. In the case of VH-SLS, the depolarized scattering intensity signal was achieved by subtracting the background intensity from the measured intensity. The background intensity was gained by measuring the signal without applying the laser light to the sample. In the case of VH-DLS, the analyzer was adjusted manually by a small rotation at each angle in order to find the optimum intensity of the anisotropic contribution (no VV contribution). Single-mode fiber optics were used (OZ, from GMP, Zurich, Switzerland) coupled to an ALV/SO-SIPD/DUAL photomultiplier with a pseudo-cross-correlation setup, ALV 5000 multiple tau digital correlator (ALV, Langen, Germany). The correlator constructed the intensity autocorrelation function $g_{VH}^{(2)}(q,t)$ of the depolarized scattered light. The regularized inverse Laplace transformation fitting procedure REPES (regularized positive exponential sum),[35,36] which directly minimizes the sum of the squared differences between the experimental and calculated $g_{VH}^{(2)}(q,t)$ and is incorporated in the GENDIST package,[37,38] was employed in the data analysis. The model used is expressed with respect to the normalized depolarized electric field correlation function $g_{VH}^{(1)}(q,t)$, which in turn is related to $g_{VH}^{(2)}(q,t)$ by Siegert's relation

$$g_{VH}^{(2)}(q,t) - 1 = \beta |g_{VH}^{(1)}(q,t)|^2 \qquad (1)$$

5480 *J. Phys. Chem. B, Vol. 113, No. 16, 2009*

Löf et al.

Here, t is the lag time and β is the coherence factor (≤ 1) that takes into account the deviations from the ideal experimental situation (perfect coherence). q is magnitude of the scattering vector, $q = (4\pi n_0/\lambda)\sin(\theta/2)$, in which n_0 is the refractive index of the medium, i.e., solvent (in this study water) for dilute solutions.

In a depolarized DLS experiment, the electric field correlation function at low q is a single-exponential function:

$$g_{VH}^{(1)}(q, t) = A\exp(-\Gamma_{VH}t) + \text{baseline} \qquad (2)$$

Here, Γ_{VH} is the depolarized relaxation frequency that consists of two parts: one that represents the translational diffusion D and another that represents the rotational diffusion Θ:

$$\Gamma_{VH} = 6\Theta + q^2 D \qquad (3)$$

Γ_{VH} was extracted from the single-modal relaxation time distribution, which was obtained from the regularized inverse Laplace transformation of the depolarized intensity correlation functions $g_{VH}^{(2)}(q,t)$ measured at various angles. By plotting Γ_{VH} as a function of q^2, the rotational diffusion coefficient was then obtained directly in the low-angle limit, $q \rightarrow 0$. Single-exponential Cumulant fits were also applied, and similar values of Γ_{VH} were obtained. However, the Laplace inversion data showed better regression values for the fits of Γ_{VH} vs q^2, and these data are thus presented in this work.

For rigid rodlike particles, the length L of the rods may be estimated from Θ by using an extended version[39] of Broersma's relation,[40] but reformulated by Tirado et al:[41]

$$\Theta = \frac{3kT}{\pi\eta_0 L^3}(\ln p + \delta) \qquad (4)$$

where $p = L/d$, in which d is the rod diameter and η_0 is the viscosity of the solvent (here water) and

$$\delta = -0.446 - \frac{0.2}{\ln 2p} - \frac{16}{(\ln 2p)^2} + \frac{63}{(\ln 2p)^3} - \frac{62}{(\ln 2p)^4} \qquad (5)$$

Small-Angle X-ray scattering. An evacuated high-performance SAXS instrument called "SAXSess" (Anton Paar KG, Graz, Austria) was used in this investigation. This instrument is a modification[42] of the so-called "Kratky compact camera".[43] The SAXSess is attached to a conventional X-ray generator (Philips, The Netherlands) equipped with a sealed X-ray tube (Cu anode target producing Cu Kα X-rays with a wavelength of 0.154 nm) operating at 40 kV and 50 mA. The samples were measured in a standard quartz capillary for the SAXSess camera (with an outer diameter of 1 mm and a wall thickness of 10 μm). The 2D scattering pattern was detected by a PI-SCX fused fiber optic taper charge-coupled device (CCD) camera from Princeton Instruments, a division of Roper Scientific, Inc. (Trenton, NJ). The used CCD detector featured a 2084 × 2084 pixel array with 24 μm × 24 μm pixel size (chip size: 50 mm × 50 mm) and was operated at −30 °C with a water-assisted cooling at 10 °C in order to reduce the thermally generated charge. Cosmic ray correction and background subtraction were performed on the 2D image before further data processing. The 2D image was integrated into the 1D scattering function $I(q)$,

corrected for the solvent-filled capillary scattering and put to an absolute scale using water as a secondary standard.[44]

The obtained SAXS spectra were further analyzed with the indirect Fourier transformation method IFT[45−47] as well as its extension, the generalized indirect Fourier transformation method GIFT.[48−50] IFT is a model-free method used for dilute particle systems with negligible particle interactions (see description in refs 45−47). For systems with nonnegligible interparticle interactions (higher concentration of the scattering particles), GIFT was employed. Assuming a dilute system of globular particles with n scattering particles per volume element, the scattered intensity can be described by the product $I(q) = nP(q)S(q)$, where $P(q)$ is the form factor representing the intraparticle scattering contributions, thus providing us with information of the particle size and shape, and $S(q)$ is the structure factor representing the interparticle contributions.

In dilute solutions, where interparticle interactions can be neglected, $S(q) = 1$; i.e., the intensity is proportional to $P(q)$. The scattering intensity from one scattering particle $I_1(q)$ can be written as the Fourier transformation of the so-called pair-distance distribution function $p(r)$ describing the geometry of the scattering particles in the real space:[46]

$$I_1(q) = 4\pi\int_0^\infty p(r)\frac{\sin(qr)}{qr}\,dr \qquad (6)$$

Here, r is the distance between two scattering centers within the particle.

The $p(r)$ function represents a histogram of the distance inside the scattering particle,[48] which means that the function adopts a value of zero at a distance r greater than the maximum dimension of the particle. Particle size and shape are therefore two important parameters that can be obtained from the $p(r)$ function. At higher concentration, where interparticle interactions have to be considered, the structure factor $S(q)$ plays an important role and contributes to the total scattered intensity. Therefore, the interparticle correlation must be taken into account during the evaluation procedure. This can be handled with the GIFT technique.[49−51] In this technique the interparticle interactions are described, in the real (r) space, by the total correlation function $h(r) = g(r) - 1$, where $g(r)$ is the radial distribution function and r is now defined as the distance between the centers of two particles.[52] As for the form factor, the connection between the q- and r-space is a Fourier transform. $S(q)$ and $h(r)$ thus form the Fourier transform pair

$$S(q) = 1 + 4\pi n\int_0^\infty h(r)r^2\frac{\sin(qr)}{qr}\,dr \qquad (7)$$

$S(q)$ can be described by a variety of models appropriate for the system under investigation. We determine $P(q)$, which remains model-free, simultaneously with the model-dependent $S(q)$ compensating for the interaction effects. The simplest structure factor model that takes into account the excluded volume effect for uncharged systems ("hard sphere model") as well as the particle polydispersity is the average structure factor $S_{ave}(q)$. This model is described by three parameters: volume fraction ϕ, interaction radius R_{HS} (radius of hard spheres), and polydispersity μ. The effective volume fraction not only takes into account the surfactants and the copolymers but also includes the bound hydrated water. For a fixed concentration, this effective volume fraction will depend on the temperature because of the different hydration states. The interaction radius
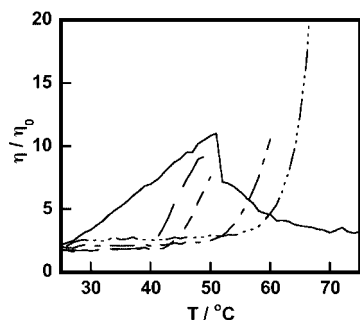
Figure 1. Relative viscosity (η/η_0, where η_0 is the water viscosity) as function of temperature for a P123−$C_{12}EO_6$ mixed micellar system at a $C_{12}EO_6$/P123 molar ratio of 2.2 (— —), 3.2 (– – –), 6.0 (– – –), and 11 (·····), as well as for a pure $C_{12}EO_6$ solution (—). The P123 concentration in the mixed solutions was kept constant at 5.0 wt %.
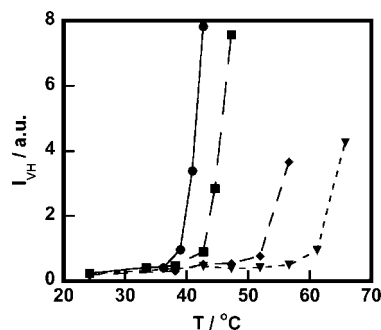

Figure 2. Depolarized light scattering intensity (I_{VH}) as a function of temperature for a dilute P123−$C_{12}EO_6$ mixed micellar system in solution at molar ratios of 2.2 (●), 3.2 (■), 6.0 (♦), and 11 (▼).

in the hard sphere model (excluded volume interaction) is close to half of the minimum center-to-center distance of the particles. The polydispersity is defined as the ratio between the width of the Gaussian size distribution σ and the particle size R_{HS} at its maximum value, i.e., $\mu = \sigma/R_{HS}$.[49]

Results and Discussion

Ultralow Shear Viscosimetry. Figure 1 displays how the viscosity, measured using the DMA instrument, of five aqueous solutions of P123−$C_{12}EO_6$ mixed micelles varied with the temperature. The values have been transferred to relative values (η/η_0) by using literature viscosity values of water. Four $C_{12}EO_6$/P123 molar ratios were investigated, 2.2, 3.2, 6.0, and 11, as well as a pure $C_{12}EO_6$ solution at 5.0 wt %. The P123 concentration in the mixed solutions was kept constant at 5.0 wt %.

For each of the investigated molar ratios, the solution viscosity η initially displayed a slight decrease with temperature (<40 °C) (the only exception was the pure $C_{12}EO_6$ solution). In this temperature regime, no significant structural changes of the mixed micelles could be observed; the size (in terms of hydrodynamic radius and molar mass) increases only mildly.[23] Hence, the steady decrease in viscosity is attributed to the viscosity decrease of the solvent (water), since the initial negative slope coincided with that for pure water (not presented). This is the reason why, for each molar ratio in Figure 1, the relative viscosity did not change significantly with temperature <40 °C (the only exception was the pure $C_{12}EO_6$ solution). This observation is in line with our previous rheology study on the same system, in which we proposed that the main reason for the observed decrease in the solution viscosity with temperature is due to the decrease in the water viscosity with temperature (see Figure 2 in ref 24). At a certain temperature, characteristic of a specific molar ratio, the relative viscosity demonstrated an abrupt increase due to the sphere-to-rod transition of the mixed micelles, as previously established by means of calorimetry, light scattering, and rheology.[22,24] In agreement with refs 22 and 24, these viscosity measurements confirmed that the sphere-to-rod transition temperature increased when the $C_{12}EO_6$/P123 molar ratio increased from 2.2 to 11. The data from differential scanning calorimetry (DSC) and isothermal titration calorimetry presented in ref 22 revealed that the shape transition of the pure P123 micelles occurred around 61 °C (this temperature depends on the PEO-PPO-PEO copolymer batch[27]). A similar viscosity increase due to a shape transition has also been detected for pure micelles of the PEO-PPO-PEO copolymers P85[53] and P94.[34]

The relative viscosity of the pure $C_{12}EO_6$ solution increased at the starting temperature of 25 °C and continued to increase until phase separation occurred. At these temperatures and concentrations, pure $C_{12}EO_6$ exist as wormlike micelles that continue to grow with increasing temperature and concentration; see, e.g., refs 23 and 54 and the references therein. In addition, it can also be seen in Figure 1 that higher molar ratios led to slightly higher initial viscosity values at 25 °C, despite the fact that the spherical mixed micelles, at higher molar ratios, were smaller prior to the shape transition.[22,23] This effect can be explained by the fact that the total concentration of the structuring material was higher for higher molar ratios. Thus, the higher the total concentration, the higher the viscosity, even though the spherical micelles are smaller.

In ref 24, the sphere-to-rod transition of the P123−$C_{12}EO_6$ mixed micelles was studied by measuring the viscosity under a specific shear rate and simultaneously increasing the temperature. The sphere-to-rod transition temperature could thereby be characterized by the minimum in the viscosity curve obtained during the temperature scan. If we define the sphere-to-rod transition as the onset of the derivative from the relative viscosity in Figure 1, the sphere-to-rod transition will appear a couple of degrees Celsius above the transition temperature that was determined with the rheological method of ref 24. The transition temperatures estimated with the DMA measurements coincided better with the values obtained from DSC as well as from the light scattering studies presented below. In the DMA measurements, the viscosity was obtained from the damping effects of the oscillating tube. This means that extremely small shear forces acted on the solution and the interaction between the mixed micelles remained practically unchanged during the measurement, as is also the case in a DSC or a light scattering experiment. On the contrary, by application of stronger shear to a solution as in a rheology experiment, the micelles are forced to collide with each other and the intermicellar interaction in the solution increases. The shape transition might therefore be induced by the shear forces, which could explain the lower transition temperatures obtained from shear rheology.[55]

Depolarized SLS. Depolarized static light scattering was performed on samples with equivalent $C_{12}EO_6$/P123 molar ratios as those in the viscosity measurements. The concentration of P123 was constant at 0.5 wt %. All measurements were carried out with the detector positioned at the scattering angle $\theta = 90°$. The analyzer in front of the detector was rotated 90°, so that only the contribution from the anisotropic scattering reached the detector. The scattering contribution from the background was subtracted afterward (see the Experimental Section). The normalized depolarized scattering intensity I_{VH} was measured as a function of temperature. In order to let the system reach equilibrium, the solutions were maintained at the measuring
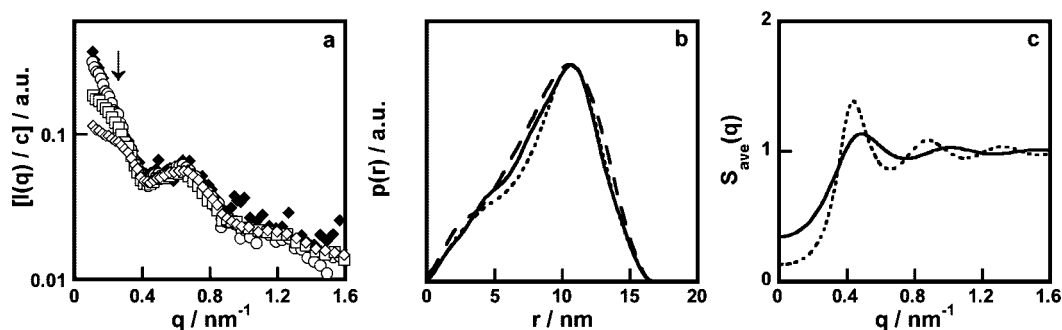
Figure 3. (a) Experimental SAXS spectra (normalized with regard to the concentration) of P123−$C_{12}EO_6$ mixed micelles for a $C_{12}EO_6$/P123 molar ratio of 2.2 at P123 concentrations of 1.0 (◆), 2.0 (○), and 10.0 wt % (□). The arrow indicates the direction of increasing concentration. All measurements were performed at 25 °C. (**b**) Corresponding pair-distance distribution functions (normalized to the same peak maximum), obtained with GIFT analysis, of the intensity spectra in (a), representing 1.0 (− − −), 5.0 (−), and 10.0 (- - - -) wt %. (c) Corresponding structure factor, obtained with GIFT analysis, of the intensity spectra of 5.0 (−) and 10.0 (- - - -) wt % from (a).

temperatures for at least 2 h before each measurement was started. Due to the crossed polarizer geometry, only micellar rods were expected to be observable in the dilute P123−$C_{12}EO_6$ micellar solution. The results are displayed in Figure 2.

It can be seen from the figure that only a very small I_{VH} signal was detected at the lower temperatures where the mixed micelles are spherical. This background comes primarily from the leakage of the polarizers. When the sphere-to-rod transition occurred, I_{VH} displayed an abrupt increase. The increasing anisotropic contribution of the light scattering therefore confirmed the growth of the mixed micelles from a spherical to a rodlike shape. It can be also noticed in Figure 2 that the transition temperature increases with increasing molar ratio. This trend has already been observed in the viscosity measurements. The resulting transition temperatures correspond well with those from previous DSC measurements.[22]

In addition, it should be pointed out that the depolarized signal increased slightly with temperature prior to the transition. One explanation for this behavior could be a structural change of the mixed micelles from a spherical to an ellipsoidal shape, since such a small anisotropic change in the micellar structure would cause a slight increase in the depolarized signal. As will be demonstrated below, the SAXS data also point in the direction of a slight ellipsoidal elongation of the mixed micelles even below the determined shape transition temperature. With increasing temperatures the PEO chains of the two amphiphiles change their conformation and the degree of hydration, thus leading to a smaller PEO head group area, which in turn decreases the interfacial curvature. Furthermore, this give rise to an intermediate structure of the mixed micelles, which lay somewhere in between the spherical and the rodlike shape. It is likely that the feature of this intermediate structure is one of an ellipsoid, since such a structure would enhance the anisotropic scattering contribution.

SAXS. SAXS experiments were performed on the P123−$C_{12}EO_6$ solutions with a fixed $C_{12}EO_6$/P123 molar ratio of 2.2 and with varying P123 concentrations (1.0, 2.0, 5.0, and 10.0 wt %). The temperature was set to 25 °C. Since a wide distribution concerning the length of the rods existed in the solutions above the shape transition (40 °C), we were unable to analyze the intensity spectra at elevated temperatures with the IFT and GIFT techniques. As a consequence, most of our analyses were restricted to measurements performed below the transition temperature. The experimental SAXS curves, the corresponding pair-distance distribution $p(r)$ functions (the Fourier transformed form factors), and the structure factors $S_{ave}(q)$ from the GIFT analyses for the mixed micellar systems are shown in Figure 3, parts a, b, and c, respectively.

The concentration-normalized intensity functions presented in Figure 3a practically overlapped, except at low q values ($q < 0.3$), where the intensity decreased with increasing concentration. This decrease reveals that the repulsive interparticle interactions increased with increasing particle concentration (a typical scattering behavior for repulsive liquid-type interactions).[56,57] The corresponding $p(r)$ functions that have been normalized for better recognition of any shape/size change with concentration are displayed in Figure 3b. The shoulder that appears on the left side of the maximum of the $p(r)$ functions suggests that the P123−$C_{12}EO_6$ mixed micelles at a $C_{12}EO_6$/P123 molar ratio of 2.2 are inhomogeneous core−shell particles, since the $p(r)$ function of a homogeneous spherical particle would have had a symmetric maximum.[49] As the inhomogeneity would increase, the $p(r)$ function would be increasingly reduced on the left side of the maximum, which was the case here. As is also shown below, for larger inhomogeneities, it was even possible to obtain a minimum in the $p(r)$ function.[49,50] Inhomogeneities inferred from Figure 3b arose from the density differences that existed between the PPO and PEO chains of the P123 copolymers as well as the alkyl chain of the $C_{12}EO_6$ molecules constituting the scattering particles. According to Figure 3b, the outer shape and size of the mixed micelles seemed to be unaffected by increasing concentration. This was concluded from the characteristic functional form of the $p(r)$ function, which indicated the presence of spherical (globular) micelles. Furthermore, the function adopted the value of 0 around 17 nm, suggesting that the diameter of the scattering particles was approximately 17 nm. This can be compared to the hydrodynamic radius of 9.1 nm (~18 nm in diameter) that was obtained for these mixed micelles by DLS at 36 °C.[22] It should be mentioned that the hydrodynamic radius found with DLS also includes the bound outer water layer, which is invisible for the X-rays. That explains the slightly lower value found in the SAXS result.

Due to the very weak interparticle interactions at 1.0 and 2.0 wt %, these two scattering curves were evaluated with a standard IFT method, where the interparticle interactions were neglected ($S(q) = 1$). In fact, the interactions were not pronounced enough in these two cases to successfully use the GIFT method. In Figure 3c, the corresponding structure factor $S_{ave}(q)$ curves are shown for concentrations at 5.0 and 10.0 wt %. They reveal that interparticle interactions have to be considered when increasing the total concentration in the mixed system at a $C_{12}EO_6$/P123 molar ratio of 2.2. Since the scattering intensity can be presented as the product of the form and the structure factor,[44] these curves explain the decreasing forward scattering that is observed with increasing concentration in Figure 3a. The

Structural Characterization of Mixed Micelles

J. Phys. Chem. B, Vol. 113, No. 16, 2009 **5483**

changes in the scattering functions with concentration therefore had their origin in the varying structure factor, namely, in the increasing interactions. Keeping in mind the results of Figure 3b, we can thus consider these systems as ones where the shape and size of the mixed micelles were unaffected by the interactions. If attention is paid to the resulting structure factor parameters, one can notice rather high volume fractions (15 and 26 %) with respect to the weight percentage of the structuring material in the samples (5.0 and 10.0 wt %, respectively). However, it is well-known that the micellar PEO corona is usually strongly hydrated, which, in turn, is expressed in the increased volume fractions.[54,57−59]

Finally, the interaction radii R_{HS} of 6.8 and 7.4 nm (for the 5.0 and 10.0 wt % solutions, respectively) that were obtained from the structure factor parameters in the GIFT analyses were smaller than the radii obtained in the corresponding $p(r)$ functions (approximately 9 nm). This may indicate an interpenetration (interdigitation) of the outer PEO chains from one micelle into the corona of another micelle. Indeed, the $p(r)$ function reflects the geometric information (size and shape) of the "visible" scattering particle or of that part of the particle that exhibits a sufficient scattering contrast to be noticed in the SAXS experiment. On the other hand, the interaction radius R_{HS} reflects the size obtained from the information on the interparticle interaction between various mixed micelles in the solution. Interdigitation therefore leads to a smaller structure factor parameter r, as one would expect from the $p(r)$ interpretation. This is a result of the micelles experiencing a distance to other micelles in the solution shorter than the value for a "contact distance" obtained from the $p(r)$ function.[60] Another explanation for this discrepancy may be the presence of hydrophilic copolymer "impurities" (with much higher PEO content than the average copolymer composition) that do not take part in the micellization process, which has been discussed in the literature[27−29] and that could influence the interaction radius.

Internal Structure from SAXS. Previous DLS and SLS measurements performed below the sphere-to-rod transition temperature have shown that a higher content of $C_{12}EO_6$ (up to a $C_{12}EO_6$/P123 molar ratio of 12) in the mixed micelles decreased their size, both in terms of the hydrodynamic radius and of the molar mass.[23] The transition temperatures were thus higher for the molar ratios above 2.2 and up to 12.[22] Indeed, a smaller sphere has a higher spontaneous curvature, and it thus demands more energy in order to change its spherical shape into a rod and thereby decreases its curvature. On the other hand, when compared to pure P123 micelles, the mixed micelles of molar ratio 2.2 demonstrated a lower sphere-to-rod transition temperature (~40 °C as opposed to ~61 °C at 1.0 wt % P123).

There are two important factors that drive the sphere-to-rod transition of pure PEO-PPO-PEO micelles. The poorer solvency of PEO in water with increasing temperature leads to a reduction of the head group area since the PEO conformation changes[64] and a decrease in the head group steric repulsion occurs. This favors growth and causes a stretching of the PPO blocks, in addition to a larger mixing of PEO with PPO, in the micellar core. The transition from a spherical to a rodlike shape will thus release this unfavorable PPO stretching.[61−63]

For P123−$C_{12}EO_6$ mixed micelles, we have previously proposed the idea that that the $C_{12}EO_6$ surfactant molecules are specifically located at the PEO/PPO interface of the micelles.[22] The observed lowering of the sphere-to-rod transition temperature is then due to a "crowding" effect at the core/corona interface (considering that the PPO core radius of the micelles is unaffected at low molar ratios up to 2.2), which causes a

decrease in the effective PEO head group area (i.e., a conformational change in a similar way as for a temperature increase,[64] and which is common for all PEO-containing amphiphilic aqueous systems[65]) and thus facilitates the shape change. This can also be rationalized in terms of the critical packing parameter; namely, the decrease of the effective PEO head group area leads to a decrease in the average packing parameter of the amphiphiles in the mixed micelle, which favors rodlike structures over spherical. In general, the critical packing parameter describes the role of a molecule's geometry in determining the self-assembled aggregate formed. It is <1/3 for a spherical micelle and between 1/3 and 1/2 for a cylindrical one.[65,66] A parallel approach to the packing parameter is the concept of mean curvature of a surfactant film.[65,67] The self-assembled aggregate adopts a curvature with the lowest energy, called the spontaneous curvature. By convention, the curvature toward the hydrophobic part is denoted as positive. In our case, the spontaneous curvature of the film of the mixed amphiphiles changes to less positive (as compared to the pure copolymer film) up to a $C_{12}EO_6$/P123 molar ratio of 2.2, which thus facilitates a sphere-to-rod transition. The same effect, i.e., the lowering of the transition temperature, due to the change in spontaneous curvature (PEO dehydration), can be reached by addition of inorganic electrolytes, such as KF or NaCl.[15,68,69]

In ref 22 it was shown, by using both DSC and visual inspection of the samples, that the sphere-to-rod transition temperature is linked to the liquid−liquid phase separation temperature (or clouding temperature); both decrease up to molar ratio 2.2, above which they increase again. These observations demonstrate the connection to the change in the spontaneous curvature of the mixed micelles. Above molar ratio 2.2, the mixed micelles decrease in radius and thus the spontaneous curvature increases (favoring spherical micelles), and as a result both the sphere-to-rod transition and phase separation temperatures increase.

As suggested in ref 22, the C_{12} part is most probably present in the PPO-rich core whereas the EO_6 part is in the hydrophilic PEO corona of the micelles. In this way, the intraparticle scattering contrast could be influenced. Since the C_{12} part is not long enough to stretch to the center of the micellar core, it resides close to the interface and affects the scattering contrast in this region, giving rise to a new cross-sectional structure. An increasing inhomogeneity with increasing $C_{12}EO_6$ content would therefore confirm that the $C_{12}EO_6$ surfactant molecules were specifically located at the interface of the micelles according to the above discussion. In order to prove this, the mixed spherical micelles were investigated using SAXS at 25 °C for all studied molar ratios, including pure P123 micelles. The P123 concentration in the solutions was 5.0 wt %. Figure 4 displays the $p(r)$ functions obtained from the GIFT analysis of the obtained SAXS intensity spectra for $C_{12}EO_6$/P123 molar ratios of 0, 2.2, 6.0, and 11.

As expected, there was a pronounced increase in the inhomogeneity with increasing amount of $C_{12}EO_6$ in the mixed micelles. This conclusion could be drawn from the increasing asymmetry observed in the $p(r)$ functions on the left side of the maximum. These $p(r)$ functions are in agreement with the example stated for inhomogeneous spheres in refs 49 and 50. A pure P123 micelle has a PPO core and a PEO corona, and since PPO and PEO are quite similar, their electron densities deviate only slightly. Similar kinds of triblock copolymer micelles have been extensively studied elsewhere; see, e.g., refs 3, 25, 38, 53, 61, 63, and 70. As can be seen also in Figure 4, the P123 micelles could be considered as slightly inhomoge-
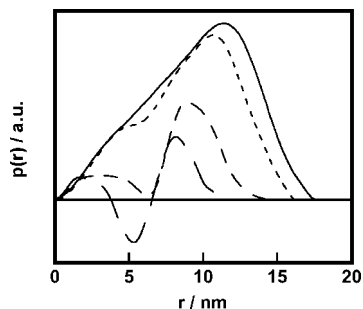
5484 *J. Phys. Chem. B, Vol. 113, No. 16, 2009*

Löf et al.

Figure 4. Pair-distance distribution functions representing the spherical shape of the P123−$C_{12}EO_6$ mixed micellar system at $C_{12}EO_6$/P123 molar ratio of 0 (i.e., pure P123) (—), 2.2 (---), 6.0 (– – –), and 11 (— —).
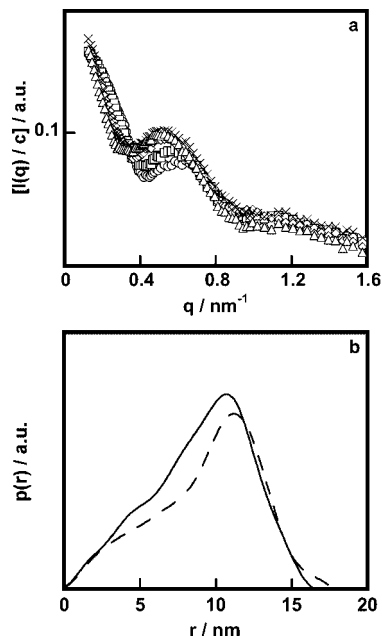

Figure 5. (a) Experimental SAXS spectra (normalized with regard to the concentration) of P123−$C_{12}EO_6$ mixed micelles at $C_{12}EO_6$/P123 molar ratio 2.2 and at temperatures of 25 (○), 30 (□), 40 (◇), 45 (×), and 50 (△) °C. The P123 concentration was 5.0 wt %. (b) Corresponding $p(r)$ functions of P123−$C_{12}EO_6$ mixed micelles for a molar ratio of 2.2 at 25 (—) and 30 (– – –) °C. At 25 °C, $\phi = 0.136$, $R = 6.14$, $\mu = 0$, and at 30 °C, $\phi = 0.102$, $R = 6.22$, $\mu = 0.013$.

neous spheres, since only a small sign of inhomogeneity arose in the corresponding $p(r)$ function. The maximum diameter that was estimated from Figure 4 for the pure P123 micelle was 18 nm. Our group has previously studied the P123 micelles with SAXS, and similar signs of small inhomogenities were then observed in the $p(r)$ functions.[14] In that case, however, the observed maximum diameter was 20 nm. The difference in diameter between the two studies was attributed to the different P123 batches used in the experiments.

The Sphere-to-Rod Transition from SAXS. Figure 5a displays the scattering intensities measured at various temperatures for the P123−$C_{12}EO_6$ mixed micelles at a $C_{12}EO_6$/P123 molar ratio of 2.2.

It was found in our previous investigations that the transition from spherical to elongated cylindrical micelles occurred around 40 °C for this molar ratio.[22,24] The scattering curves in Figure 5a conform to these results (all curves were cut off for $q > 1.5$ nm^{-1}, since the values at higher q range had no significance). The scattering curves up to 40 °C, which were expected to represent the globular micelles before the transition, gradually

shifted toward lower q values with increasing temperature. At temperatures above 40 °C, the scattering peak around 0.5 nm^{-1} remained constant with increasing temperature, but the innermost upturn in the scattering curves still demonstrated an inward shift. The constant position of the scattering peak above 40 °C suggested that once the micelles started to elongate (grow in one dimension), the cross section of these rodlike micelles remained practically unchanged. The upturn in the scattering curves and the inward shifts at low q values indicate that a further growth of the cylinder length took place with increasing temperature.[56] The sphere-to-rod transition was thus clearly shown also in the results from SAXS and confirmed those from the VH-SLS experiments, as well as the results of the viscosity measurements.

Figure 5b displays the corresponding $p(r)$ functions obtained from the data at 25 and 30 °C. These functions suggest that the scattering particles are inhomogeneous and that the overall size was practically the same in both cases. The curves were more or less identical up to approximately 16 nm, after which a slight shoulder could be observed in the case of the 30 °C result. Such a shoulder could be an indication of the start of the early particle growth. The two curves also revealed that the internal scattering contrast of the particles changed with increasing temperature, which explains the differences in the experimental SAXS curves in Figure 5a prior to the transition. One explanation for the change in contrast is that, at higher temperatures, water has left the outer parts of the micellar PEO corona (dehydration) due to the PEO groups undergoing conformational changes to a less polar configuration.[64] As we already mentioned, it is well-known that the PEO corona contains a lot of water, especially in the outermost part, which reduces its scattering contrast considerably.[57,58] This outermost part of the hydrated PEO corona can therefore be difficult to discern with SAXS.

The resulting values of the structure factor parameters obtained with the GIFT evaluation clearly show that the effective volume fraction, ϕ, of the scattering particles decreased from 14 % at 25 °C to 10 % at 30 °C. Since the micelles occupy a smaller volume at 30 °C as opposed to at 25 °C, the interparticle interactions were reduced, as was observed in the $S_{ave}(q)$ curves (not presented). Furthermore, the polydispersity parameter μ, obtained from the GIFT fit, increased slightly when the temperature was increased from 25 to 30 °C (see legend of Figure 5b). Together with the small shoulder observed at high r values for the $p(r)$ function at 30 °C, this could represent an indication of the start of an early elongation of the scattering particles into ellipsoidal shapes.[57,58] This would also explain the slightly increasing depolarized signal below 40 °C in Figure 2. As discussed previously (Figure 3c), the values of the interaction radius, R_{HS} (half-center-to-center distance), were smaller than the estimated radii from the $p(r)$ functions also in this case. The obtained interaction radius R_{HS} was, however, slightly larger at 30 °C (6.22 nm) as compared to the one obtained at 25 °C (6.14 nm). This difference might be due to increased interpenetration difficulties due to the outer layers dehydrating and becoming more compact.

Depolarized DLS. In order to further explore the structure of the P123−$C_{12}EO_6$ mixed micelles, VH-DLS experiments were performed. The purpose was to determine the hydrodynamic length of the rodlike micelles from the rotational diffusion coefficient in a similar way as in refs 38 and 71 for pure PEO-PPO-PEO block copolymer micelles. In a VH-DLS experiment, only the anisotropic scattering is collected. In this system, anisotropic scattering occurred when the spherical micelles changed their structure into rods, as shown in Figure 2.
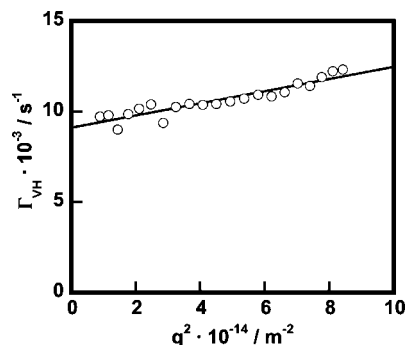
Structural Characterization of Mixed Micelles

J. Phys. Chem. B, Vol. 113, No. 16, 2009 **5485**

Figure 6. Decay rate Γ_{VH} vs q^2 from depolarized DLS measurements on a P123–$C_{12}EO_6$ mixed micellar system with a $C_{12}EO_6$/P123 molar ratio of 2.2 and 0.5 wt % with respect to P123. The measurement temperature was 43 °C. The solid line is a linear least-squares fit.

VH-DLS experiments were carried out on the mixed solution of $C_{12}EO_6$/P123 molar ratio 2.2 at 43 °C. According to DSC, this is 3 °C above the sphere-to-rod transition for this mixture.[22] The P123 concentration in the solution was 0.5 wt %. Figure 6 presents Γ_{VH} as a function of q^2.

The data points in Figure 6 fit a linear function representing a sum contribution of translational and rotational diffusion. The fact that this linear fit does not go through the origin is clear evidence of an anisotropy of the mixed micelles at 43 °C.[38] From the intercept in Figure 6, the rotational diffusion coefficient could be determined to $\Theta = 1520$ s^{-1}. Equations 4 and 5 were used, and the average length L of the rods was estimated to 102 nm. This gave a p value of 6, indicating that the use of the two equations was justified. Reference 22 describes the calculation of the length from the measured translational diffusion coefficient, D_0, at infinite dilution obtained from polarized DLS by using another model by Broersma[40] also reformulated by Tirado et al.[41] According to these calculations, the length was estimated to be 107 nm (not 104, which is a misprinted value presented in ref 22). In the former DLS study, the hydrodynamic radius of the spherical mixed micelles (estimated at 36 °C) was used, which corresponded to a radius of 9.1 nm. By employing the same equation for the translational diffusion data measured here but inserting the diameter obtained from the SAXS experiments (17 nm), L could now be calculated to 112 nm. The calculated values from the translational diffusion were close to the value estimated with the rotational diffusion coefficient (102 nm). It should be pointed out that the measured quantity Θ in the VH-DLS experiments scaled with L^{-3} and was therefore more sensitive to changes in L than in the diameter d. However, the choice of model used to calculate the length of the rod from the rotational or the translational diffusion coefficient played a more significant role in estimating the length. All models were based on Broersma's relation,[40] but they have been refined and reformulated by other groups to be valid for various ranges of p.[71–73] The reason why we chose this particular set of equations was that they were valid in a p range suitable for the mixed rodlike micelles studied here.

Conclusions

A thorough characterization of P123–$C_{12}EO_6$ mixed micelles in solution at various $C_{12}EO_6$/P123 molar ratios was performed with techniques such as ultralow shear viscosimetry, depolarized light scattering, and SAXS. The two first techniques were employed, in particular, to follow the sphere-to-rod transition. The transition temperatures coincided with previously published results obtained by DSC, light scattering, and rheology, thus suggesting an increasing transition temperature with an increasing content of $C_{12}EO_6$ in the mixed micelles.[22,24] Well-established methods of IFT and GIFT were utilized to analyze the SAXS data. These methods proved to be very powerful in their task and contributed to our knowledge of the mixed micelles with respect to the interparticle level. IFT was used to obtain the $p(r)$ function in the diluted regime, but for concentrations above 2 wt % the interparticle interactions had to be taken into account and thus the GIFT evaluation was applied. By utilizing GIFT, not only the shape and size but also the interparticle interactions could be explored at various molar ratios. It was observed that an increasing content of $C_{12}EO_6$ in the mixed micelles increased the inhomogeneities. This strongly supported the previous anticipation of $C_{12}EO_6$ organizing in the interface between the PPO-based core and the PEO-based corona, with the C_{12} alkyl chain stretching into the hydrophobic core and the EO_6 part residing in the hydrophilic corona.[22]

Due to the resolution limits of the instrument and the high polydispersity of the length of the rodlike mixed micelles, it was not possible to analyze the SAXS data above the transition temperature with the reported analysis methods. Nevertheless, the evolution of the sphere-to-rod transition could be clearly seen from the scattering intensity curves and matches the expected changes in the particle geometry during the increase in temperature. The constant position of the scattering peak around 0.5 nm^{-1} confirmed that the cross-sectional radius after the transition remained unchanged when the temperature was further increased. Moreover, the innermost upturn in the scattering curves, which continued to shift inward with temperature, was clear evidence of increasing structural changes with temperature, most likely into an elongated structure. The depolarized scattering intensity I_{VH} in combination with the $p(r)$ functions suggested structural changes, prior to the determined sphere-to-rod transition temperatures, of the spherical mixed micelles into what was most likely slightly ellipsoidal-shaped micelles.

VH-DLS was used to study the rotational diffusion in order to obtain the mean length of the rods at 43 °C for mixed micelles at a molar ratio of 2.2. Broersma's relation reformulated by Tirado et al. appeared to be a good model,[41] and the average rod length could be estimated to be 102 nm. This value agreed well with previously published results, where the length was obtained from the translational diffusion coefficient at 40 °C.[22]

References and Notes

(1) Alexandridis, P. *Curr. Opin. Colloid Interface Sci.* **1996**, *1*, 490.
(2) *Amphiphilic Block Copolymers: Self-Assembly and Applications*; Alexandridis, P., Lindman, B., Eds.; Elsevier: Amsterdam, 1997.
(3) Mortensen, K. *Colloids Surf., A* **2001**, *183–185*, 277.
(4) Kabanov, A. V.; Alakhov, V. Y. *Crit. Rev. Theor. Drug Carrier Syst.* **2002**, *19*, 1.
(5) Fusco, S.; Borzacchiello, A.; Netti, P. A. *J. Bioact. Comp. Polym.* **2006**, *21*, 149.
(6) Almgren, M.; van Stam, J.; Lindblad, C.; Li, P.; Stilbs, P.; Bahadur, P. *J. Phys. Chem.* **1991**, 5677.
(7) Hecht, E.; Mortensen, K.; Gradzielski, M.; Hoffmann, H. *J. Phys. Chem.* **1995**, *99*, 4866.
(8) Li, Y.; Xu, R.; Bloor, D. M.; Holzwarth, J. F.; Wyn-Jones, E. *Langmuir* **2000**, *16*, 10515.
(9) Li, Y.; Xu, R.; Coudrec, S.; Bloor, D. M.; Wyn-Jones, E.; Holzwarth, J. F. *Langmuir* **2001**, *17*, 183.
(10) Li, Y.; Xu, R.; Coudrec, S.; Bloor, D. M.; Holzwarth, J. F.; Wyn-Jones, E. *Langmuir* **2001**, *17*, 5742.

5486 *J. Phys. Chem. B, Vol. 113, No. 16, 2009*

Löf et al.

(11) da Silva, R. C.; Olofsson, G.; Schillén, K.; Loh, W. *J. Phys. Chem. B* **2002**, *106*, 1239.

(12) Thurn, T.; Couderc, S.; Sidhu, J. S.; Bloor, D. M.; Penfold, J.; Holzwarth, J. F.; Wyn-Jones, E. *Langmuir* **2002**, *18*, 9267.

(13) Jansson, J.; Schillén, K.; Olofsson, G.; da Silva, R. C.; Loh, W. *J. Phys. Chem. B* **2004**, *108*, 82.

(14) Jansson, J.; Schillén, K.; Nilsson, M.; Söderman, O.; Fritz, G.; Bergmann, A.; Glatter, O. *J. Phys. Chem. B* **2005**, *109*, 7073.

(15) Ganguly, R.; Aswal, V. K.; Hassan, P. A.; Gopalakrishnan, I. K.; Kulshreshtha, S. K. *J. Phys. Chem. B* **2006**, *110*, 9843.

(16) De Lisi, R.; Gradzielski, M.; Lazzara, G.; Milioto, S.; Muratore, N.; Prevost, S. *J. Phys. Chem. B* **2006**, *110*, 25883.

(17) Kumbhakar, M. *J. Phys. Chem. B* **2007**, *111*, 14250.

(18) Couderc-Azouani, S.; Sidhu, J.; Thurn, T.; Xu, R.; Bloor, D. M.; Penfold, J.; Holzwarth, J. F.; Wyn-Jones, E. *Langmuir* **2005**, *21*, 10197.

(19) Sastry, N. V.; Hoffmann, H. *Colloids Surf., A* **2004**, *250*, 247.

(20) Coudrec, S.; Li, Y.; Bloor, D. M.; Holzwarth, J. F.; Wyn-Jones, E. *Langmuir* **2001**, *17*, 4818.

(21) Hossain, K. M.; Hinata, S.; Lopez-Quintela, A.; Kunieda, H. *J. Dispersion Sci. Technol.* **2003**, *24*, 5742.

(22) Löf, D.; Niemiec, A.; Schillén, K.; Loh, W.; Olofsson, G. *J. Phys. Chem. B* **2007**, *111*, 5911.

(23) Schillén, K.; Jansson, J.; Löf, D.; Costa, T. *J. Phys. Chem. B* **2008**, *112*, 5551.

(24) Löf, D.; Schillén, K.; Torres, M.; Müller, A. J. *Langmuir* **2007**, *23*, 11000.

(25) Alexandridis, P.; Hatton, T. A. *Colloids Surf., A* **1995**, *96*, 1.

(26) Brown, W.; Schillén, K.; Hvidt, S. *J. Phys. Chem.* **1992**, *96*, 6038.

(27) Batsberg, W.; Ndoni, S.; Trandum, C.; Hvidt, S. *Macromolecules* **2004**, *37*, 2965.

(28) Hvidt, S.; Batsberg, W. *Int. J. Polym. Anal. Charact.* **2007**, 12–13.

(29) Mortensen, K.; Batsberg, W.; Hvidt, S. *Macromolecules* **2008**, *41*, 1720.

(30) Costa, T.; Schillén, K.; Miguel da, G. M.; Lindman, B.; Seixas de Melo, J. *J. Phys. Chem. B*, in press.

(31) Wanka, G.; Hoffmann, H.; Ulbricht, W. *Macromolecules* **1994**, *27*, 4145.

(32) Olofsson, G. *J. Phys. Chem.* **1985**, *89*, 1473.

(33) Strey, R.; Pakusch, A. In *Surfactants in Solution*; Mittal, K. L., Bothorel, P., Eds.; Plenum Publishing Corporation: New York, 1987; Vol. 4, p 465.

(34) Fritz, G.; Glatter, O. *J. Phys. Chem. B* **2000**, *104*, 3463.

(35) Štěpánek, P. In *Dynamic Light Scattering: The Method and Some Applications*; Brown, W., Ed.; Oxford University Press: Oxford, 1993; p 177.

(36) Jakěs, J. *Collect. Czech. Chem. Commun.* **1995**, *60*, 1781.

(37) Johnsen, R. M.; Brown, W. In *Laser Light Scattering in Biochemistry*; Harding, S. E., Sattelle, D. B., Bloomfield, V. A., Eds.; The Royal Society of Chemistry, Thomas Graham House, Science Park: Cambridge, U.K., 1992; p77.

(38) Schillén, K.; Brown, W.; Johnsen, R. M. *Macromolecules* **1994**, *27*, 4825.

(39) Broesma, S. *J. Chem. Phys.* **1981**, *74*, 6989.

(40) Broesma, S. *J. Chem. Phys.* **1960**, *32*, 1632.

(41) Tirado, M.; Lopéz Martinez, C.; de la Torre, J. G. *J. Chem. Phys.* **1984**, *81*, 2047.

(42) Bergmann, A.; Orthaber, D.; Scherf, G.; Glatter, O. *J. Appl. Crystallogr.* **2000**, *33*, 869.

(43) Kratky, O.; Stabinger, H. *Colloid Polym. Sci.* **1984**, *262*, 345.

(44) Orthaber, D.; Bergmann, A.; Glatter, O. *J. Appl. Crystallogr.* **2000**, *33*, 218.

(45) Glatter, O. *Acta Phys. Austriaca* **1977**, *47*, 83.

(46) Glatter, O. *J. Appl. Crystallogr.* **1977**, *10*, 415.

(47) Glatter, O. *J. Appl. Crystallogr.* **1980**, *13*, 577.

(48) Glatter, O. *J. Appl. Crystallogr.* **1979**, *12*, 166.

(49) Brunner-Popela, J.; Glatter, O. *J. Appl. Crystallogr.* **1997**, *30*, 431.

(50) Weyerich, B.; Brunner-Popela, J.; Glatter, O. *J. Appl. Crystallogr.* **1999**, *32*, 197.

(51) Fritz, G.; Glatter, O. *J. Phys.: Condens. Matter* **2006**, *18*, S2403.

(52) Hansen, J. P.; McDonald, I. R. *The Theory of Simple Liquids*; Academic: London, 1990.

(53) Glatter, O.; Scherf, G.; Schillén, K.; Brown, W. *Macromolecules* **1994**, *27*, 6046.

(54) Glatter, O.; Fritz, G.; Lindner, H.; Brunner-Popela, J.; Mittelbach, R.; Strey, R.; Egelhaaf, S. U. *Langmuir* **2000**, *16*, 8692.

(55) Saito, S.; Koizumi, S.; Matsuzaka, K.; Suehiro, S.; Hashimoto, T. *Macromolecules* **2000**, *33*, 2153.

(56) Glatter, O.; Strey, R.; Schubert, K. V.; Kaler, E. W. *Ber. Bunsen-Ges. Phys. Chem.* **1996**, *100*, 323.

(57) Tomšič, M.; Bešter-Rogač, M.; Jamnik, A.; Kunz, W.; Touraud, D.; Bergmann, A.; Glatter, O. *J. Phys. Chem. B* **2004**, *108*, 7021.

(58) Tomšič, M.; Bešter-Rogač, M.; Jamnik, A.; Kunz, W.; Touraud, D.; Bergmann, A.; Glatter, O. *J. Colloid Interface Sci.* **2006**, *292*, 194.

(59) Lindner, H.; Scherf, G.; Glatter, O. *Phys. Rev. E* **2003**, *67*, 0614021.

(60) Glatter, O.; Orthaber, D.; Stradner, A.; Scherf, G.; Fanun, M.; Nissim, G.; Clément, V.; Leser, M. E. *J. Colloid Interface Sci.* **2001**, *241*, 215.

(61) Mortensen, K. *Macromolecules* **1993**, *26*, 805.

(62) Linse, P. *J. Phys. Chem.* **1993**, *97*, 13896.

(63) Mortensen, K. *Polym. Adv. Technol.* **2001**, *12*, 2.

(64) Karlström, G. *J. Phys. Chem.* **1985**, *89*, 4962.

(65) Jönsson, B.; Lindman, B.; Holmberg, K.; Kronberg, B. *Surfactants and Polymers in Aqueous Solution*; John Wiley & Sons Ltd: Chichester, England, 2003.

(66) Israelachvili, J. *Intermolecular and Surface Forces*, 2nd ed.; Academic Press Ltd: London, 1992.

(67) Evans, D. F.; Wennerström, H. *The Colloidal Domain Where Physics, Chemistry, Biology, and Technology Meet,* 2nd ed.; John Wiley & Sons, Inc: New York, 1999.

(68) Jörgensen, E. B.; Hvidt, S.; Brown, W.; Schillén, K. *Macromolecules* **1997**, *20*, 2355.

(69) Ganguly, R.; Aswal, V. K.; Hassan, P. A. *J. Colloid Interface Sci.* **2007**, *315*, 693.

(70) Pedersen, J. S.; Gerstenberg, M. C. *Colloids Surf., A* **2003**, *213*, 175.

(71) Lehner, D.; Lindner, H.; Glatter, O. *Langmuir* **2000**, *16*, 1689.

(72) Newman, J.; Swinney, H. L.; Day, L. A. *J. Mol. Biol.* **1977**, *116*, 593.

(73) de Souza Lima, M. M.; Wong, J. T.; Paillet, M.; Borsali, R.; Pecora, R. *Langmuir* **2003**, *19*, 24.